International Geology Review, Vol. 48, 2006, p. 443–465.

Geological and Geochemical Characteristics of Granitoids in the Eastern Tauride Belt, Southeastern Turkey

ÖZCAN DUMANLILAR,[1]

General Directorate of Mineral Research and Exploration (MTA), Mineral Research and Exploration Department, 06520, Balgat-Ankara, Turkey

DOGAN AYDAL,

Ankara University, Faculty of Engineering, Geological Engineering Department, 06100, Beşevler-Ankara, Turkey

HALIDE DUMANLILAR,

General Directorate of Mineral Research and Exploration (MTA), Mineral Analysis and Technology Department, 06520, Balgat-Ankara, Turkey

AND PINAR ALICI ŞEN

General Directorate of Mineral Research and Exploration (MTA), Mineral Research and Exploration Department, 06520, Balgat-Ankara, Turkey

Abstract

As a consequence of plate convergence and continental collision, widespread magmatism occurred in the Malatya-Elazig area of the eastern Tauride belt. Igneous activities in the study area can be subdivided into two separate phases, the Baskil and Bilaser Tepe complexes. The present study particularly focuses on these granitoid associations.

The Late Cretaceous granitoid associations exhibit calc-alkaline and tholeiitic major-oxide trends. Baskil granitoids consist primarily of quartz, plagioclase, and hornblende, with relatively lesser amounts of orthoclase. Bilaser Tepe granitoids are mainly composed of quartz, orthoclase, plagioclase, hornblende, and biotite. Oxides and apatite are common accessory phenocrysts in both granitoids. Based on petrographic and bulk-rock geochemical data, Baskil granitoids are classified as quartz-diorite, quartz-monzodiorite, and tonalite, whereas Bilaser Tepe granitoids are granodiorite and tonalite. Both units have peraluminous and metaluminous compositions.

Trace-element plots indicate that the Baskil granitoids have geochemical features similar to I-type granitoids derived from island-arc settings. The Bilaser Tepe granitoids exhibit both I- and S-type characteristics, suggesting a post-collisional origin. Baskil magmatism is interpreted as arc magmatism related to Late Cretaceous convergence between the Keban microcontinent and the southern branch of Neo-tethys. This magmatic phase was followed by collision between the Keban microcontinent and the Bitlis-Pütürge massif. Continental collision resulted in crustal thickening. Subsequently, the Bilaser Tepe granitoids were intruded, signifying post-collisional tectonic setting in the Malatya-Elazig area. Consequently, the petrological and geochemical data are consistent with the geodynamic model of the eastern Taurus.

Introduction

LATE CRETACEOUS MAGMATIC ROCKS in the study area crop out in an area from Hakkari to Elbistan in the eastern Tauride belt (Fig. 1). In previous studies, Yazgan (1984) and Asutay (1988) argued that these magmatic rocks were products of arc magmatism. Bingöl (1984) and Akgül (1991) proposed that igneous rocks in the study area formed during two major stages: 1) as products of arc magmatism between the southern branch of the Neo-tethys and the Keban microcontinent; and 2) as products of continental collision between the Bitlis-Pütürge massif and the magmatic arc. Akgül and Bingöl (1997) and Dumanlilar et al. (1999) argued that the magmatic rocks in Ispendere (Malatya) and at Piran village (Keban) were derived from a common island-arc setting, with

[1]Corresponding author; email: ozcand@demirexport.com

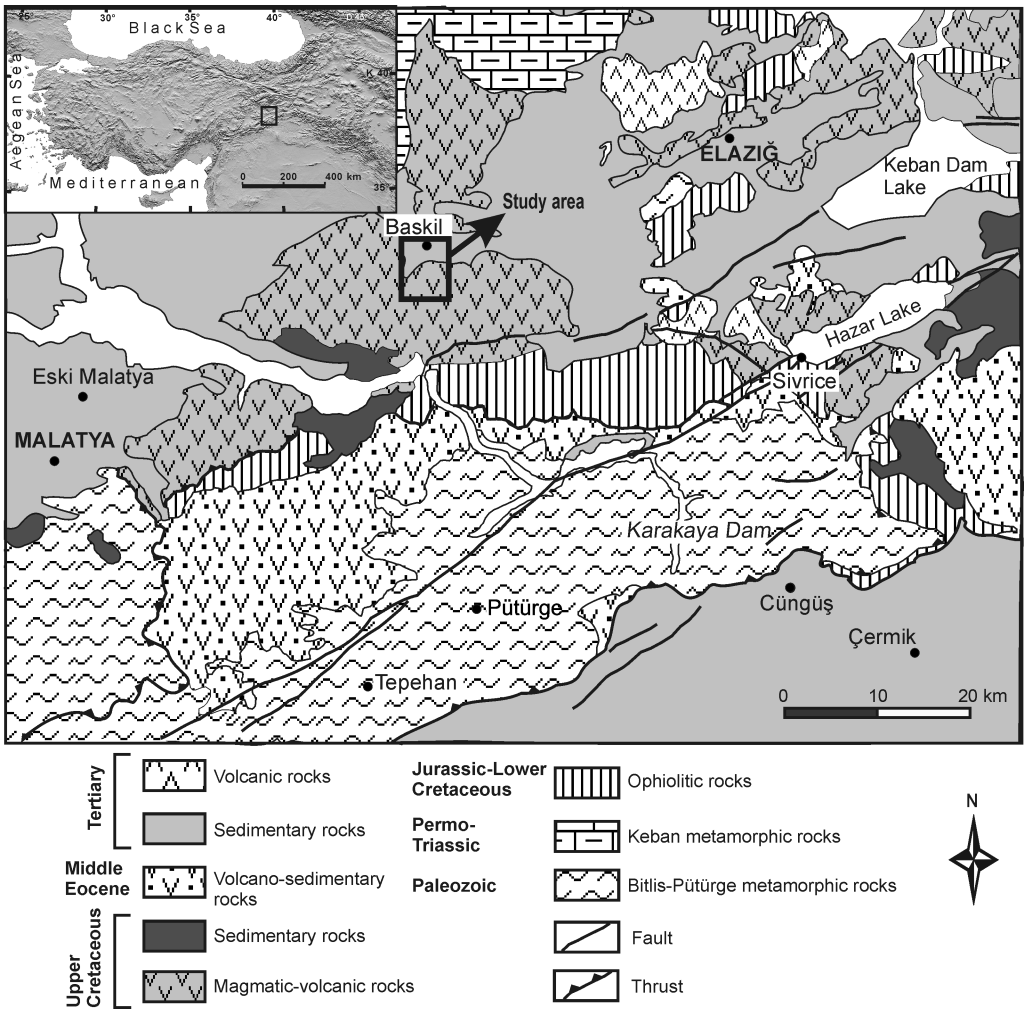

FIG. 1. Regional geological and location maps of the study area (simplified from the 1:500,000 scale map available from the General Directorate of Mineral Research and Exploration (MTA, 2002).

significant features of I-type and magnetite-series granitoids.

Tectonic evolution of the eastern Taurus involved an arc-continent collision between the Keban microcontinent and Arabian plate during the Late Cretaceous. Northward motion of the Afro-Arabian plate caused subduction during Eocene to Miocene time, followed by continental collision between the Eurasian and Arabian plates during the middle to late Miocene. The continental collision led to thickening and shortening of the continental crust in eastern Anatolia (Şengör, 1980; Şengör and Yilmaz, 1981; Fytikas et al., 1984; Yilmaz et al., 1998), with a N-S–directed compressional regime that continues today.

The principal objective of this paper is to present new geochemical data and approaches to the understanding of the geodynamics and source characteristics of magmatism in the Malatya-Elazig area of the eastern Tauride belt. This study is particularly focused on the geochemistry of granitoid associations of the Malatya-Elazig area.

For this purpose, a detailed geologic map of a 77 km^2 area was prepared at a scale of 1:100.000. During field work, 126 samples were collected for mineralogical and petrographical determinations.

Major, trace, and rare-earth elements were chemically analyzed in 26 samples of magmatic rocks at MTA laboratories and Acme Analytical Laboratories in Canada. Whole-rock major oxides and trace elements were analyzed by ICP (inductively coupled plasma) and XRF (X-ray fluorescence) methods, whereas analyses of rare-earth elements (REE) were conducted by the ICP-MS (mass spectrometry) method. In this study, we also used the analyses of six samples (5 tonalite/granodiorite, 1 diorite) collected by Asutay (1985) from the Baskil magmatites.

Numerous studies of the geological, tectonic, petrographic, and petrological aspects of the study area and its surroundings have been previously undertaken (Yazgan, 1972, 1981, 1984; Asutay and Turan, 1986; Beyarslan, 1991; Akgül, 1991; Yazgan and Chessex, 1991; Herece et al., 1992; Dumanlilar, 1993, 1998; Turan et al., 1995).

Geological Setting

The study area, situated south of Baskil, is dominated by Late Cretaceous magmatic rocks (Asutay, 1985), and Pleistocene and Holocene sedimentary units (Fig. 1). Outside the study area, Late Cretaceous magmatic rocks have tectonic contacts with the Kömürhan ophiolite to the southeast, whereas they intrude the Keban metamorphics to the north. Furthermore, it has been shown that to the southwest, dacite-porphyry of the Bilaser Tepe magmatites cuts the upper Campanian–lower Maastrichtian Sagdiçlar Formation. All these units are unconformably overlain by Late Cretaceous and Tertiary sediments (Fig. 2).

The Baskil and Bilaser Tepe magmatic rocks were first defined by Perinçek (1979). Various researchers who had worked elsewhere in the eastern Taurides (Perinçek, 1979; Turan, 1984; Bingöl, 1988; Dumanlilar, 1998) defined them collectively as the Yüksekova Complex. The same magmatic rocks were named the Baskil magmatites by Asutay (1985), the Baskil magmatic rocks by Yazgan et al. (1987), and the Elazig magmatites by Akgül and Bingöl (1997). Herece et al. (1992) suggested that Late Cretaceous magmatites cropping out in the vicinity of Elazig developed at two different time intervals; the first was defined as the Baskil Magmatic Complex, and the second as the Pertek Magmatic Complex. Throughout this work, magmatic rocks near Baskil have been mapped as two distinct units, namely the Baskil and Bilaser Tepe granitoids.

Baskil magmatic rocks

In the study area, the first phase of the Baskil magmatic rocks is represented by dioritic rocks. The subsequent acidic phase is of tonalitic composition. The studies of Akgül and Bingöl (1997) near Keban, and those of Dumanlilar (1998) near Malatya, proposed that magmatism was initiated as a basic phase and later shifted to an acidic phase.

Asutay (1985), who originally examined magmatic rocks near Baskil, claimed that regional magmatic rocks show gradual transitions to one another and divided them into four groups: (1) diorite-monzodiorite; (2) a transition group (quartz-diorite); (3) granodiorite-tonalite; and (4) monzonite. He also regarded andesitic and basaltic volcanic rocks as the final products of the Baskil magmatism.

The Baskil magmatic rocks are seen to have tectonic relationships with the Kömürhan ophiolite to the south outside the study area. The plutonic rocks of the Baskil magmatites display intrusive contacts with ophiolites farther south around Karga Dagi, and near Ispendere (east of Malatya). The Sagdiçlar Formation of Late Campanian–Early Maastrichtian age transgressively rests upon this unit. Around Keban, the intrusive rocks of the Baskil magmatites show contact-metamorphic effects along their contacts with the Keban metamorphics of Permo-Triassic age (Özgül, 1981). K-Ar radiometric dating of the Baskil magmatites has yielded a Coniacian–Santonian age of 83.5–86 Ma (Yazgan et al., 1987).

In the study area, Baskil magmatites are represented by quartz-diorite, quartz-monzodiorite, and tonalite. Thus, henceforth we will refer to these as the Baskil granitoids.

Quartz-diorite crops out over an area stretching from the southern part of the Badem Tepe–Hemik Tepe line to Cansizhimik Mahallesi, and is surrounded by units of the Bilaser Tepe magmatites (Fig. 3). Quartz-monzodiorite crops out around Bejikan Ziyareti Tepe. It has a lighter green color than the quartz diorite and is characterized by coarser grain size. Tonalite, exposed in extreme northwestern part of the study area, is distinguished by its greyish white–dirty white color and coarse (up to 1 cm) grain size, with elliptical or rounded quartz grains having vitreous luster.

Bilaser Tepe magmatic rocks

Granitic rocks, defined by earlier workers as belonging to later phases of the Baskil magmatites, are re-evaluated here as the Bilaser Tepe magmatites, and were considered as a separate phase

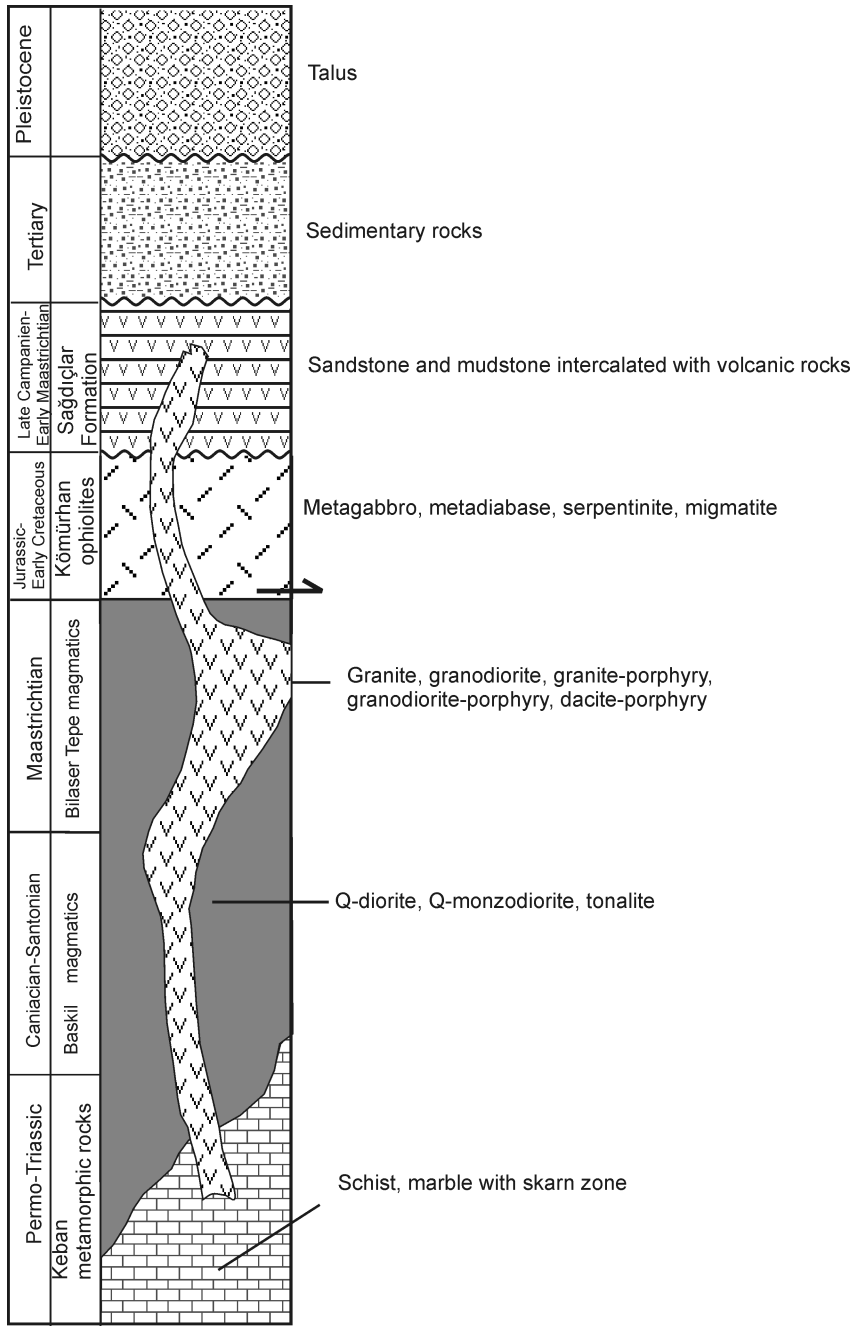

FIG. 2. Generalized columnar section for the study area.

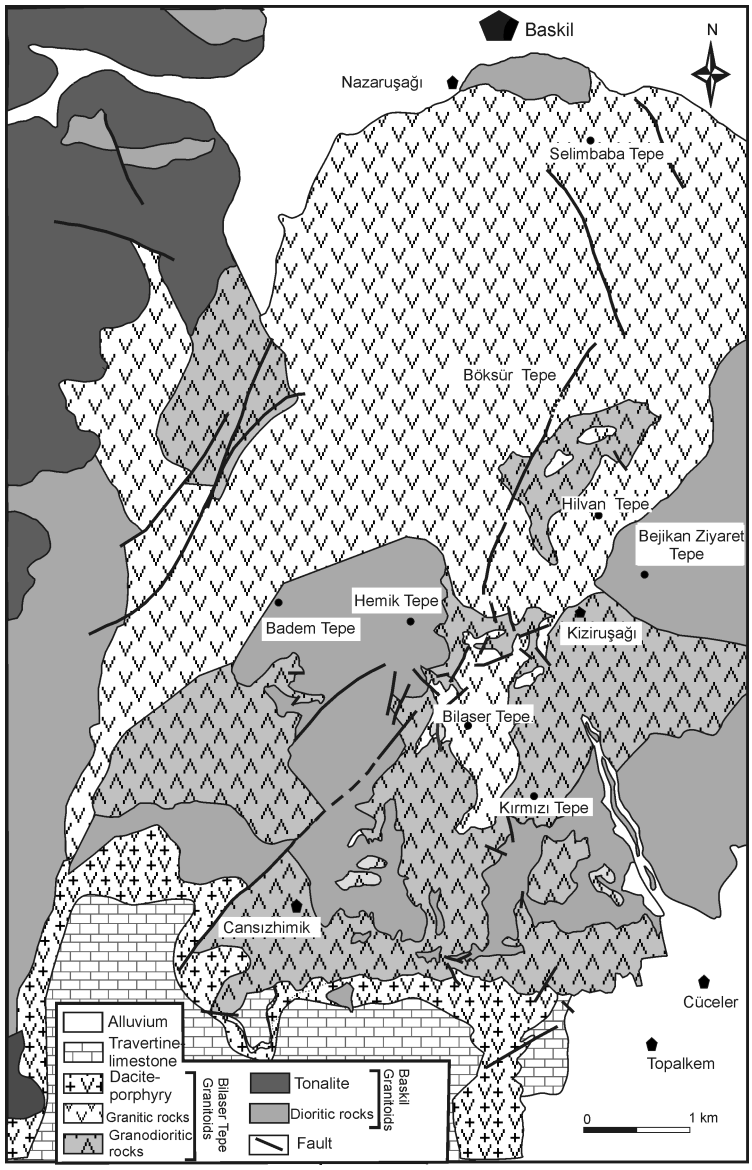

FIG. 3. Generalized geological sketch map of the study area (simplified from Dumanlilar, 2002).

throughout the present study on the basis of field, petrographic, and geochemical data. The Bilaser Tepe magmatites have intrusive contacts with the Baskil magmatites and comprise five different phases, namely, granite, granodiorite, granite-porphyry, granodiorite-porphyry, and dacite-porphyry.

The outermost granite crops out over an area extending from the northern side of the Badem Tepe-Hemik Tepe-Kiziruşagi Mahallesi line of the Baskil flatland (Fig. 3). It is easily distinguished by its typical pinkish color. Rocks of this unit are characterized with N80°E/30°NE joint set, and by their pinkish white arenated appearance. Aplite veins 10 to 50 cm thick occur with variable orientations in these granites. At Bilaser Tepe, granite-porphyry occurs at the center and grades outward to grano-

TABLE 1. Modal Mineralogical Composition of Representative Samples from the Baskil Granitoids[1]

Sample no.	Components, %					
	Q	Alk. feld.	Plag	Hbl	Chlorite	Oxides
			Dioritic rocks			
BY10	1.2	–	54.6	37.4	–	6.8
BY11	4.2	–	51.5	39.1	–	5.2
T22	11.8	–	53.7	32.0	2.2	0.3
KA8	3.7	8.5	42.9	43.0	1.9	–
KA7	4.9	7.1	38.9	46.8	2.3	–
			Tonalite			
T28	43.9	–	49.85	–	6.25	–
T21	40.1	–	54.1	–	5.8	–
T24	58.9	–	37.7	–	2.6	0.8

[1]Abbrevations: Q = Quartz; Alk.feld.= alkali feldspar; Plag = plagioclase; Hbl = hornblende.

diorite with gradual transitions between these rock types.

Granodiorite crops out to the south of Kiziruşagi Mahallesi and to the north of Cansizhimik Mahallesi (Fig. 3). This unit, which has intrusive contacts with diorite and granite of the Baskil magmatites, locally occurs as 1 to 20 m thick veins within them. It is greyish green in outcrop and has a finer grained texture than the other units of the Bilaser Tepe magmatites. Hand specimens contain finer-grained bladed crystals of mafic minerals, which are dispersed between grayish-white feldspar and vitreous quartz crystals.

Greyish white granite porphyry forms the central part of the Bilaser Tepe magmatites. It is readily distinguished from the other units by its higher quartz content and lack of mafic minerals.

Granodiorite porphyry crops out in a narrow zone northwest of Kiziruşagi Mahallesi (Fig. 3). The mafic mineral content of this unit is higher than that of the granodiorite unit, and other components (except for alkali feldspar) have a smaller grain size. Alkali feldspar reaches up to 2 cm in size.

The EW-trending dacite-porphyry, the latest phase of the Bilaser Tepe magmatites, crops out south of Cansizhimik Mahallesi. The dacite-porphyry, the youngest unit in the study area, shows gradual transitions with granodiorite of the Bilaser Tepe magmatites to the north, and has intrusive contacts with units of the Baskil magmatites to the west. The eastern margin is overlain by younger sediments. The dacite-porphyry has intrusive contacts with the Sagdiçlar Formation (Late Campanian–Early Maastrichtian), consisting of alternating mudstone, siltstone, and limestone, with volcanic claystone along their southern margins (outside the study area).

In this study, we particularly focus on the granitic and granodioritic rocks of the Bilaser Tepe magmatites. Thus, hereinafter we refer to these granitic and granodioritic rocks as the Bilaser Tepe granitoids.

Petrography

Baskil granitoids

The modal mineralogical compositions of selected samples from the Baskil granitoids are listed in Table 1. Petrographic and modal mineralogical investigations demonstrate that the Baskil granitoids are composed of quartz diorite, quartz monzodiorite, and tonalite (Fig. 4).

Quartz diorite has holocrystalline subhedral equigranular textures. Modal mineralogical analyses (Table 1) represent quartz (Q), plagioclase (pl), hornblende (hb) and oxides as percentages of the quartz diorite volume. The primary mineralogical components of these rocks are plagioclase and hornblende. Poikilitic hornblende enclosing plagioclase occurs as clear euhedral to subhedral phenocrysts. Oxides and apatite are characteristic accessory minerals.

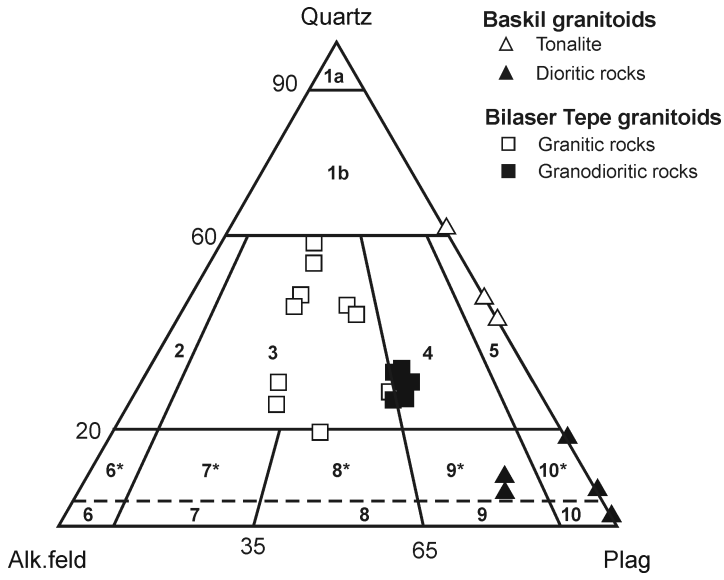

FIG. 4. Modal mineralogical nomenclature for the Baskil and Bilaser Tepe granitoids on the "quartz–alkali feldspar–plagioclase" diagram of Streckeisen (1976).

Quartz monzodiorite occurs as holocrystalline subhedral equigranular textures. Modal mineralogical analyses (Table 1) show that quartz (Q), alkali feldpar (Alk.feld), plagioclase (Plag), hornblende (Hbl), chlorite, and oxides make up significant percentages of the quartz monzodiorite volume. The most abundant minerals in the quartz monzodiorite are plagioclase, orthoclase, hornblende with accessory apatite, and oxide minerals. Plagioclase is represented by euhedral phenocrysts rimmed by alkali feldspar. Orthoclase is euhedral and perthitic, with rare plagioclase inclusions and Carlsbad twins. The Q-diorite and Q-monzodiorite are grouped as dioritic rocks and thus will be referred to as dioritic rocks in subsequent sections.

Tonalite, with holocrystalline subhedral equigranular texture, is mainly composed of quartz, plagioclase, and hornblende phenocrysts. Hornblende is altered to chlorite. Plagioclase is oligoclase to andesine in composition. Modal mineralogical analyses (Table 1) represent quartz, plagioclase, and chlorite as percentages of the tonalite volume.

Bilaser Tepe granitoids

The modal mineralogical compositions of selected samples from the Bilaser Tepe granitoids are listed in Table 2. Petrographic and modal mineralogical investigations demonstrate that these rocks comprise granite and granodiorite (Fig. 4). In the study area, two types of granitic rocks can be distinguished on the basis of their textural features: granite and granite porphyry.

Granite, which exhibits holocrystalline subhedral equigranular texture, is composed of quartz, orthoclase, plagioclase, amphibole, biotite, and apatite grains. Orthoclase occurs as clear euhedral phenocryts and is perthitic with quartz inclusions and carlsbad twins. Smoky to dark gray quartz phenocryst forms anhedral grains. Plagioclase phenocrysts are euhedral and are characterized by zoning and corrosion features. They are oligoclase in compositon.

Granite porphyry exhibits holocrystalline porphyry texture. Euhedral to subhedral quartz and plagioclase are the most abundant phenocrysts, but locally orthoclase and biotite phenocryts also are associated. Quartz, plagioclase, orthoclase, and biotite are also present as microcrysts in the groundmass. Quartz and plagioclase microcrysts in the groundmass occur as anhedral and euhedral to subhedral grains, respectively. Most of the quartz phenocrysts contain irregular alkali feldspar, plagioclase, and tourmaline inclusions. Compositionally, the plagioclase phenocrysts are andesine. Orthoclase is euhedral to subhedral as

TABLE 2. Modal Mineralogical Composition of Representative Samples from the Bilaser Tepe Granitoids[1]

Sample no.	Components, %					
	Q	Alk. feld	Plag	Hbl	Bio	Oxides
			Granite			
BY16	23.5	44.9	24.8	6.8	–	–
N18	29.2	44.7	24.2	1.1	0.8	–
BY13	17.4	38.6	33.3	10.2	–	0.5
N2	44.0	24.4	28.0	3.6	–	–
D29	25.0	24.0	41.0	10.0	–	–
N2-1	42.0	23.6	30.4	4.0	–	–
TS7-2P	57.8	24.5	16.5	–	1.2	–
TS2-P33	53.4	26.5	18.4	–	1.4	0.3
TS2-P26	47.6	32.4	19.6	–	0.4	–
TS3-P10	45.2	34.8	19.6	–	0.4	–
			Granodiorite			
BF-5	28.5	21.4	39.6	–	7.9	2.6
TS3-P6	25.3	19.9	39.7	–	14.5	0.6
TS-31	22.2	22.8	40.0	5.4	8.6	1.0
KA-6	27.2	19.8	44.2	6.3	2.5	–
N1	21.7	20.1	40.4	7.4	7.8	2.6
TS-17	28.0	21.2	41.8	1.8	6.6	0.6
TS-35	27.6	18.7	38.4	2.4	12.4	0.5

[1]Abbrevations: Q = Quartz; Alk.feld.= alkali feldspar; Plag = plagioclase; Hbl = hornblende; Bio = biotite.

both phenocrysts and microcrysts, and Carlsbad twins are typical.

Granite and granite porphyry are grouped as granitic rocks and thus will be referred to as granite in the following sections. Modal mineralogical analyses (Table 2) of the granitic rocks reveal that quartz, alkali feldspar, plagioclase, hornblende, biotite, with relatively lesser amounts of oxides comprise significant percentages of the granite volume. Two types of granodioritic rocks are distinguished on the basis of their textural features: granodiorite and granodiorite porphyry.

Granodiorite, having a subhedral equigranular texture, mainly consists of quartz, plagioclase, biotite, and hornblende phenocrysts. Apatite, zircon, titanite, and oxides are common accessory mineral phases. Quartz and plagioclase occur as anhedral and euhedral phenocrysts, respectively. Euhedral to subhedral orthoclase typically displays Carlsbad twins, and poikilitic orthoclase enclosing plagioclase, biotite, and amphibole also occurs as larger grains.

Granodiorite porphyry has holocrystalline porphyrytic textures, and is comprised of orthoclase, plagioclase, quartz, biotite, and hornblende as essential phases, as well as apatite, zircon, and oxides as accessories. Biotite and hornblende occur as anhedral phenocrysts, and also occur as inclusions in orthoclase phenocrysts.

Mafic magmatic enclaves of various size (centimeters to meters) are abundant in the Bilaser Tepe granitoids. Enclaves in the granites are ellipsoidal in shape, microgranular in texture, and Q-diorite in composition, and are mainly composed of hornblende and plagioclase, with lesser amounts of alkali feldspar and quartz, with apatite, oxides, and titanite as accessories. Plagioclase occurs as subhedral phenocrysts and microlites. Quartz occurs as clear anhedral phenocrysts. Alteration is common in hornblende laths and alkali feldspar crystals, and they are highy chloritized, carbonatized, and sericitized, respectively.

The mineralogical composition of enclaves in the granodiorite porphyry is identical to that of the host

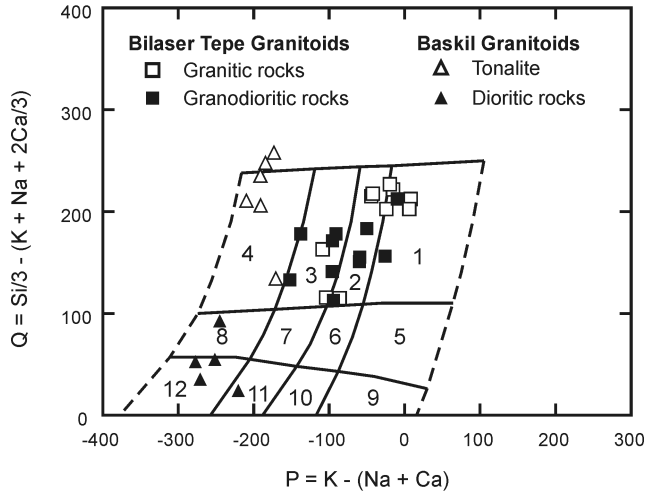

FIG. 5. Q = [(Si/3 – (K + Na + 2Ca/3)] vs P = [K – (Ca + Na)] diagram for the Baskil and Bilaser Tepe granitoids (Debon and Le Fort, 1988).

rock. These enclaves, displaying porphyritic texture, are made up of alkali feldspar, quartz, biotite, and hornblende, with apatite and oxides as accessories.

Geochemistry

Major-oxide geochemistry

Major-oxide, trace-, and rare-earth element analyses of representative samples from Bilaser Tepe and Baskil granitoids are listed in Table 3. In general, the SiO_2 contents of both groups of granitoids range from 45 to 77%. In the Q = [(Si/3 – (K + Na + 2Ca/3)] versus P = [K – (Ca + Na)] plot (Fig. 5), commonly used for discrimination of granitoids (Debon and Le Fort, 1988), the Bilaser Tepe granitoids range in composition from granodiorite to granite, whereas the Baskil granitoids plot in the gabbro, monzogabbro, and Q-diorite fields. Petrographic observations demonstrate that these rocks, termed gabbro on the basis of their chemistries, have dioritic mineralogies. Therefore, data from the Bilaser Tepe and Baskil granitoids were plotted on the A = [Al – (K + Na + 2Ca)] versus B = (Fe + Mg + Ti) diagram (Debon and Le Fort, 1988). As shown in Figure 6, the dioritic rocks of the Baskil granitoids are displaced along the hornblende and biotite line, possibly indicating their dioritic rather than gabbroic nature. Consequently, the geochemical nomenclature of the Bilaser Tepe and Baskil granitoids is compatible with the "Q-alk feld-plag" ternary discrimination diagram of Streckeisen (1976) (Fig. 4). Analyses of almost all samples from the Baskil and Bilaser Tepe granitoids plot in the subalkaline field of the Irvine and Baragar (1971) diagram. Subalkaline samples from the Bilaser Tepe and Baskil granitoids exhibit calc-alkaline and both calc-alkaline and tholeiitic signatures, respectively (Fig. 7).

Based on normative mineralogical and geochemical data, the Baskil and Bilaser Tepe granitoids can be distinguished as two different chemical groups. The most diagnostic features of the Baskil and Bilaser Tepe granitiods are their different K_2O/Na_2O ratios. The K_2O/Na_2O ratios of the Baskil granitoids range from 0.04 to 0.65, indicating their sodic nature, whereas the Bilaser Tepe granitoids generally have K_2O/Na_2O ratios greater than 1, indicating a more potassic nature than the Baskil granitoids. CIPW norms for the granitoids indicate that the Bilaser Tepe granitoids have peraluminous and metaluminous compositions, containing normative corundum (0.26 to 3.32 wt%) and diopside (0.18 to 4.38 wt%), respectively. The presence of corundum may reflect the contribution of crustal material to the magma. The Baskil granitoids are mostly metaluminous and contain normative diopside (0.30 to 20.05 wt%).

Plots of SiO_2 versus selected major oxides are shown in Figure 8. Increasing SiO_2 is well correlated with decreasing MgO, Fe_2O_3, CaO, Al_2O_3, and TiO_2. These variations correspond to those expected from fractional crystallization. For instance, MgO

TABLE 3. Major-Oxide, Trace-, and Rare-Earth Element Analyses of Representative Samples from the Baskil and Bilaser Tepe Granitoids

	Bilaser Tepe granitoids, granitic rocks									
Sample no.	BY13	BY16	D29	N2	N2-1	TS2-P26	TS7-2P	TS3-P10	TS2-P33	N18
					wt%					
SiO_2	65.15	66.54	66.85	74.66	74.8	74.72	76.79	74.22	74.08	74.76
Al_2O_3	14.75	15.2	14.82	12.33	12.32	12.56	12.27	11.98	12.72	12.94
Fe_2O_3	6.3	5.03	5.06	3.44	3.5	2.69	1.89	3.29	3.22	2.82
MgO	1.22	0.98	1.55	0.25	0.26	0.14	0.1	0.15	0.22	0.17
CaO	3.44	3.06	1.95	1.48	1.48	0.9	0.66	0.96	0.95	0.94
Na_2O	3.84	3.87	4.03	3.11	3.05	2.87	3.11	2.59	2.73	3.25
K_2O	3.9	4.43	2.81	3.92	3.91	4.41	4.38	5.11	5.24	4.59
TiO_2	0.36	0.29	0.29	0.16	0.16	0.09	0.07	0.08	0.1	0.12
P_2O_5	0.11	0.09	0.05	0.01	0.01	0.01	0.01	0.01	0.01	0.01
MnO	0.13	0.1	0.07	0.06	0.06	0.03	0.02	0.03	0.04	0.05
LOI	0.6	0.2	2.4	0.4	0.4	1.4	0.5	1.3	0.4	0.2
Total	99.8	99.79	99.88	99.82	99.95	99.82	99.8	99.72	99.71	99.85
					wt%					
Quartz	15.63	16.5	23.27	35.77	36.19	37.66	39.28	35.48	33.66	34.09
Orthoclase	23.45	26.5	17.19	23.46	23.37	26.63	26.2	30.87	31.37	27.38
Albite	32.96	33.05	35.16	26.56	26.01	24.74	26.55	22.34	23.33	27.67
Anorthite	11.66	11.12	9.78	7.47	7.46	4.63	3.34	4.94	4.85	4.78
Corundum	0	0	1.73	0.26	0.36	1.43	1.21	0.42	0.81	0.89
Diopside	4.38	3.27	0	0	0	0	0	0	0	0
Hypersthene	11.04	8.88	12.24	6.21	6.33	4.79	3.32	5.84	5.84	5.01
Olivine	0	0	0	0	0	0	0	0	0	0
Apatite	0.27	0.22	0.12	0.02	0.02	0.02	0.02	0.02	0.02	0.02
Ilmenite	0.69	0.56	0.57	0.31	0.31	0.17	0.13	0.15	0.19	0.23
Zircon	0.04	0.03	0.04	0.02	0.03	0.02	0.02	0	0.02	0.02
					ppm					
Rb	161.78	204.6	159.82	192.27	198.51	189.07	204.88	204	217	213.5
Sr	210.9	212.1	124.1	107.7	113.1	73.1	68.6	68	83	95.6
Zr	203.5	161.5	211.9	121.6	125.3	94.5	108.7	1.8	99	105.5
Y	33.2	24.1	25.4	15.4	15.9	10.5	7	0.3	11	11.9
Nb	21.88	16.86	15.65	23.06	23.81	14.06	12.95	68	22	18.14
Ba	349	414	331	312	311	434	276	469	454	433
Ga	19.4	18.1	17.7	16.5	17.3	13.8	15.4	204	–	16.4
Hf	5.2	4.1	4.9	3.5	3.6	2.9	3.3	0.01	3	3.1
Ta	1.6	1.2	1.1	1.8	1.9	1.3	1.3	27	2.5	1.4
Th	14.1	22.6	18.6	20.5	20.9	19.6	13	93	24.5	23.3
Tl	1	1	1.9	0.5	0.4	0.6	0.5	10		0.5
U	4.5	6.2	7.1	7.3	7.5	6.7	8.3	35.8	14.3	5.9
La	28.8	27.9	49.5	32.8	33.8	27.3	14.5	35.8	27.5	30.1
Ce	62.2	51.9	82.3	56.3	57.9	44.7	22.6	33	32	48.5
Pr	7.5	5.77	8.63	5.92	5.9	4.32	2.5	–	–	4.91
Nd	25.8	19.8	27.7	18.8	19	13.3	7.4	13	14	14.8
Sm	5.2	3.6	5.2	3.1	3	2	1.3	1.8	1.5	2.2
Eu	0.76	0.68	0.95	0.43	0.41	0.31	0.22	0.3	0.4	0.3
Gd	4.76	3.3	4.55	2.34	2.4	1.5	1	–	–	1.77
Tb	0.79	0.56	0.73	0.38	0.38	0.21	0.15	0.21	0.21	0.29
Dy	5.58	3.92	4.62	2.54	2.59	1.53	1.03	–	–	2.05
Ho	1.18	0.82	0.88	0.54	0.56	0.32	0.22	–	–	0.41
Er	3.79	2.78	2.51	1.56	1.65	1.09	0.72	–	–	1.32
Tm	0.65	0.45	0.39	0.29	0.27	0.19	0.13	–	–	0.22
Yb	4.11	2.97	2.48	1.8	2.14	1.23	1.1	1.6	1.5	1.72
Lu	0.63	0.43	0.37	0.28	0.3	0.21	0.17	0.26	0.25	0.23
A/CNK	0.88	0.91	1.12	1.02	1.03	1.13	1.11	1.04	1.07	1.07

Table continues

TABLE 3. *continued*

Sample no.	Bilaser Tepe granitoids, granodioritic rocks										
	N1	TS-17	TS-31	TS-35	Bf-5	KA6	TS3-P6	K1	K3	K5	K2
						wt%					
SiO_2	70.35	67.19	66.8	67.04	70.7	66.7	68.71	76.07	72.09	66.61	69.5
Al_2O_3	14.74	15.13	14.94	15.1	15.6	15.7	15.46	12.35	13.87	15.66	14.4
Fe_2O_3	3.88	4.55	3.96	4.38	2.6	4.67	4.54	2.29	3.2	4.94	3.9
MgO	0.64	1.02	0.76	1.08	0.3	0.61	1.13	0.17	0.55	1.03	0.6
CaO	1.74	1.78	3.51	2.41	1.2	2.59	2.28	0.63	1.64	2.51	1.7
Na_2O	4.09	3.51	4.42	3.28	4.2	4.26	4.24	3.13	3.4	3.88	3.2
K_2O	3.24	4.1	2.66	4.25	3.2	4.26	2	4.83	4.21	3.58	5.1
TiO_2	0.24	0.36	0.31	0.32	0.2	0.27	0.25	0.05	0.21	0.26	0.3
P_2O_5	0.05	0.09	0.66	0.07	0.1	0.08	0.03	0.01	0.01	0.1	0.1
MnO	0.05	0.11	0.07	0.09	0.1	0.1	0.04	0.04	0.05	0.07	0.1
LOI	0.8	0.9	0.7	1.2	1.95	0.7	1	0.4	0.7	1.2	0.55
Total	99.82	98.74	98.79	99.22	100.15	99.94	99.68	99.97	99.93	99.84	99.45
						wt%					
Quartz	27.11	23.26	21.75	22.42	29.94	16.36	27.06	36.23	29.81	20.39	24.55
Orthoclase	19.47	24.94	16.13	25.8	19.35	25.58	12.07	28.82	25.23	21.63	30.67
Albite	35.09	30.5	38.28	28.44	36.28	36.49	36.52	26.66	29.08	33.45	27.48
Anorthite	8.59	8.63	13.4	11.96	5.52	11.27	11.41	3.2	8.37	12.22	8.13
Corundum	1.43	1.89	0	0.85	3.32	0	2.26	0.81	0.7	1.03	0.7
Diopside	0	0	0.18	0	0	1.21	0	0	0	0	0
Hypersthene	7.81	9.93	8.15	9.8	5	8.46	10.16	4.23	6.47	10.63	7.74
Olivine	0	0	0	0	0	0	0	0	0	0	0
Apatite	0.12	0.22	1.61	0.17	0.24	0.19	0.07	0.02	0.02	0.24	0.24
Ilmenite	0.46	0.7	0.6	0.62	0.39	0.52	0.48	0.1	0.4	0.5	0.58
Zircon	0.03	0.05	0.04	0.04	0.04	0.04	0.03	0.02	0.03	0.03	0.05
						ppm					
Rb	138.97	149	85	153	93	218.08	99	218.65	183.16	171.92	174
Sr	224.4	231	331	213	121	255.2	136	72	184.4	223.6	163
Zr	171.5	221	196	199	209	193	160	76.5	145.6	165.4	244
Y	19.3	26	23	24	14	22.9	16	9.7	21.7	37.7	33
Nb	17.49	40	20	32	22	20.22	22	14.96	30.24	44.83	57
Ba	296	300	305	347	221	320	142	338	505	415	639
Ga	18	–	–	–	–	20.7	–	15.8	20.6	23.3	–
Hf	4.2	–	–	–	–	4.3	4	2.6	3.8	4.3	–
Ta	1.2	–	–	–	–	1.3	0.5	1.5	2.4	4	–
Th	17.5	12			–	17.2	18.7	28.6	21.8	19	–
Tl	0.4	–	–	–	–	0.5	–	1.5	0.6	0.8	–
U	5.5	–	–	–	–	3.3	5.9	7.6	6.7	8.3	–
La	41	–	–	–	–	40.2	34	29.8	38.7	30.3	–
Ce	67.9	–	–	–	–	67.4	43	49.4	68.3	61.3	–
Pr	6.87	–	–	–	–	7.17	–	4.94	7.33	7.62	–
Nd	21.9	–	–	–	–	23.5	11	14.7	24.3	28.5	–
Sm	3.4	–	–	–	–	3.9	2.7	2.2	4.6	6.3	–
Eu	0.59	–	–	–	–	0.79	0.5	0.25	0.74	0.78	–
Gd	2.62	–	–	–	–	3.27	–	1.66	3.87	6.11	–
Tb	0.42	–	–	–	–	0.52	0.5	0.26	0.61	0.99	–
Dy	3.03	–	–	–	–	3.75	–	1.6	3.89	6.47	–
Ho	0.62	–	–	–	–	0.76	–	0.35	0.72	1.26	–
Er	2.06	–	–	–	–	2.49	–	1.25	2.16	3.8	–
Tm	0.33	–	–	–	–	0.41	–	0.23	0.36	0.64	–
Yb	2.34	–	–	–	–	2.95	1.8	1.61	2.42	4.4	–
Lu	0.37	–	–	–	–	0.42	0.25	0.26	0.34	0.6	–
A/CNK	1.10	1.12	0.90	1.05	1.24	0.96	1.16	1.07	1.05	1.06	1.04

Table continues

TABLE 3. *continued*

Sample no.	Baskil granitoids, dioritic rocks				Baskil granitoids, tonalite					
	BY10	B11	KA7	806	TS21	T24	65	73	815	827
					wt%					
SiO_2	45.5	48.3	44.8	47.64	76.2	73	66.8	74.3	73.22	73.57
Al_2O_3	19.23	14.8	15	16.96	13.18	13.8	15.3	12.1	13.93	12.87
Fe_2O_3	11.26	12.6	17	9.99	2.3	3.5	3.5	2.4	3.09	2.7
MgO	7.39	6.6	6	7.35	0.55	0.7	1.07	0.85	1.1	0.84
CaO	13.52	8.6	11	11.55	2.75	3.6	4.7	3.3	2.08	3.29
Na_2O	1.09	3.1	1.7	2.3	3.98	4.6	4.13	3.91	5.1	4.14
K_2O	0.25	2	0.5	0.88	0.27	0.2	2.36	0.28	0.57	0.26
TiO_2	0.5	0.6	1.1	0.62	0.19	0.2	0.21	0.25	0.44	0.27
P_2O_5	0.01	0.1	0.1	0.08	0.01	0.1	–	–	0.07	0.04
MnO	0.16	0.3	0.2	0.22	0.03	0.1	0.071	0.051	0.07	0.09
LOI	1	2	0.85	–	0.4	0.05	0.77	–	–	–
Total	99.92	99	98.25	97.59	99.86	99.85	98.91	97.441	99.67	98.07
					wt%					
Quartz	0	0	0	0	44.02	34.77	21.33	42.03	33.6	39.31
Orthoclase	1.52	12.37	3.1	5.39	1.61	1.19	14.26	1.7	3.4	1.57
Albite	9.43	20.92	15.03	19.62	33.94	39.14	35.73	34.03	43.43	35.82
Anorthite	47.92	21.49	33.26	34.55	13.76	16.53	16.75	15.08	10	16.14
Corundum	0	0	0	0	1.35	0	0	0	1.3	0
Diopside	17.1	18.81	19.55	20.05	0	0.74	7.05	1.54	0	0.29
Hypersthene	6.94	0	6.28	0	4.95	7.04	4.87	5.15	7.29	6.27
Olivine	16.13	21.53	20.38	18.73	0	0	0	0	0	0
Apatite	0.02	0.25	0.25	0.2	0.02	0.24	0	0	0.17	0.1
Ilmenite	0.97	1.19	2.18	1.22	0.36	0.38	0.41	0.49	0.84	0.52
Zircon	0	0.02	0.01	0.01	0.02	0.02	0	0	0.02	0.02
					ppm					
Rb	13.96	60	29	19	11.67	5	–	–	12	5
Sr	26	223	100	113	60	100	2527	76	82	71
Zr	14.7	105	30	30	87.4	85	–	–	96	99
Y	8.6	19	11	20	8.6	13	17	33	37	33
Nb	1.1	20	20	2	1.11	20	–	–	2	2
Ba	200.2	291	158	237	195.4	180	893	115	168	123
Ga	16.7	–	–	16	14.4	–	–	–	15	13
Hf	0.4	–	–	–	2.3	–	–	–	–	–
Ta	0.4	–	–	–	0.2	–	–	–	–	–
Th	0.4	–	–	–	0.7	–	–	–	–	–
Tl	0.4	–	–	–	0.3	–	–	–	–	–
U	0.2	–	–	–	0.4	–	–	–	–	–
La	1.8	4.4	–	–	4.4	–	–	–	–	–
Ce	3.6	8.5	–	–	8.5	–	–	–	–	–
Pr	0.59	1.29	–	–	1.29	–	–	–	–	–
Nd	2.5	5.1	–	–	5.1	–	–	–	–	–
Sm	0.9	1.2	–	–	1.2	–	–	–	–	–
Eu	0.4	0.58	–	–	0.58	–	–	–	–	–
Gd	1.26	1.23	–	–	1.23	–	–	–	–	–
Tb	0.22	0.21	–	–	0.21	–	–	–	–	–
Dy	1.76	1.41	–	–	1.41	–	–	–	–	–
Ho	0.38	0.3	–	–	0.3	–	–	–	–	–
Er	1.17	1.01	–	–	1.01	–	–	–	–	–
Tm	0.16	0.16	–	–	0.16	–	–	–	–	–
Yb	1.05	1.22	–	–	1.22	–	–	–	–	–
Lu	0.16	0.19	–	–	0.19	–	–	–	–	–
A/CNK	0.72	0.65	0.64	0.66	1.11	0.96	0.85	0.95	1.09	0.98

[1]Total iron is expressed as Fe_2O3; LOI= loss on ignition.

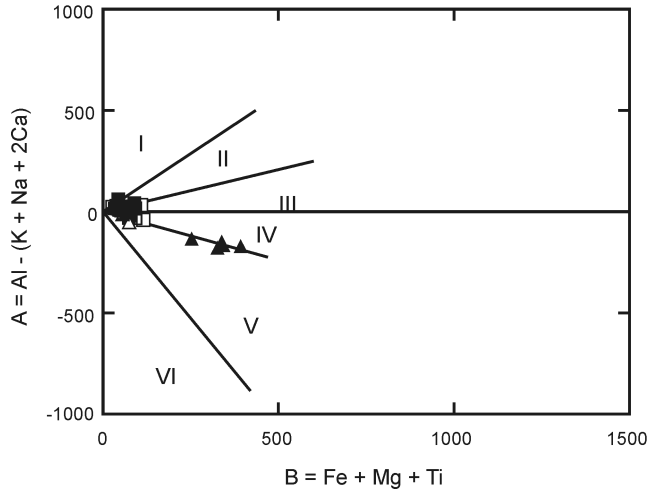

FIG. 6. A = [Al – (K + Na + 2Ca)] vs B = (Fe + Mg + Ti) diagram for the Baskil and Bilaser Tepe granitoids (Debon and Le Fort, 1988). Symbols are the same as those in Figure 4.

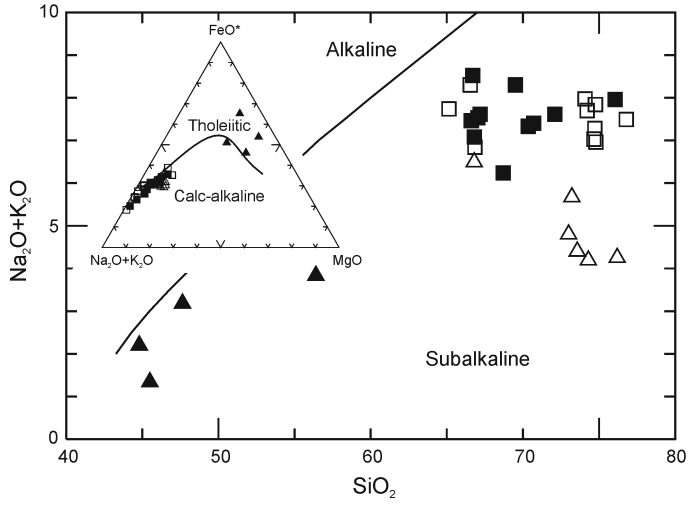

FIG. 7. SiO_2 vs $Na_2O + K_2O$ diagram for the Baskil and Bilaser Tepe granitoids (Irvine and Baragar, 1971). Inset shows the AFM diagram of Irvine and Baragar (1971). Symbols are the same as those in Figure 4.

and Fe_2O_3 decrease regularly with increasing SiO_2. These variations are compatible with fractionation of olivine, clinopyroxene, and Fe-Ti oxides. Decrease of CaO, Al_2O_3, and TiO_2 reflects crystallization of clinopyroxene, Ca-plagioclase, and Fe-Ti oxides, respectively. The overall trends in the SiO_2 variation diagrams seem to be consistent with the processes of fractional crystallization.

The ASI-Fe_{tot} diagram of Norman et al. (1992) indicates that the Baskil granitoids typically represent I-type granite features (Fig. 9), whereas the Bilaser Tepe granitoids exhibit mostly I-type granite characteristics and—to a relatively lesser extent—S-type granite characteristics.

The Bilaser Tepe granitoids range in major-oxide ratios as follows: $Na_2O/CaO < 5.0$; $Na_2O/K_2O =$

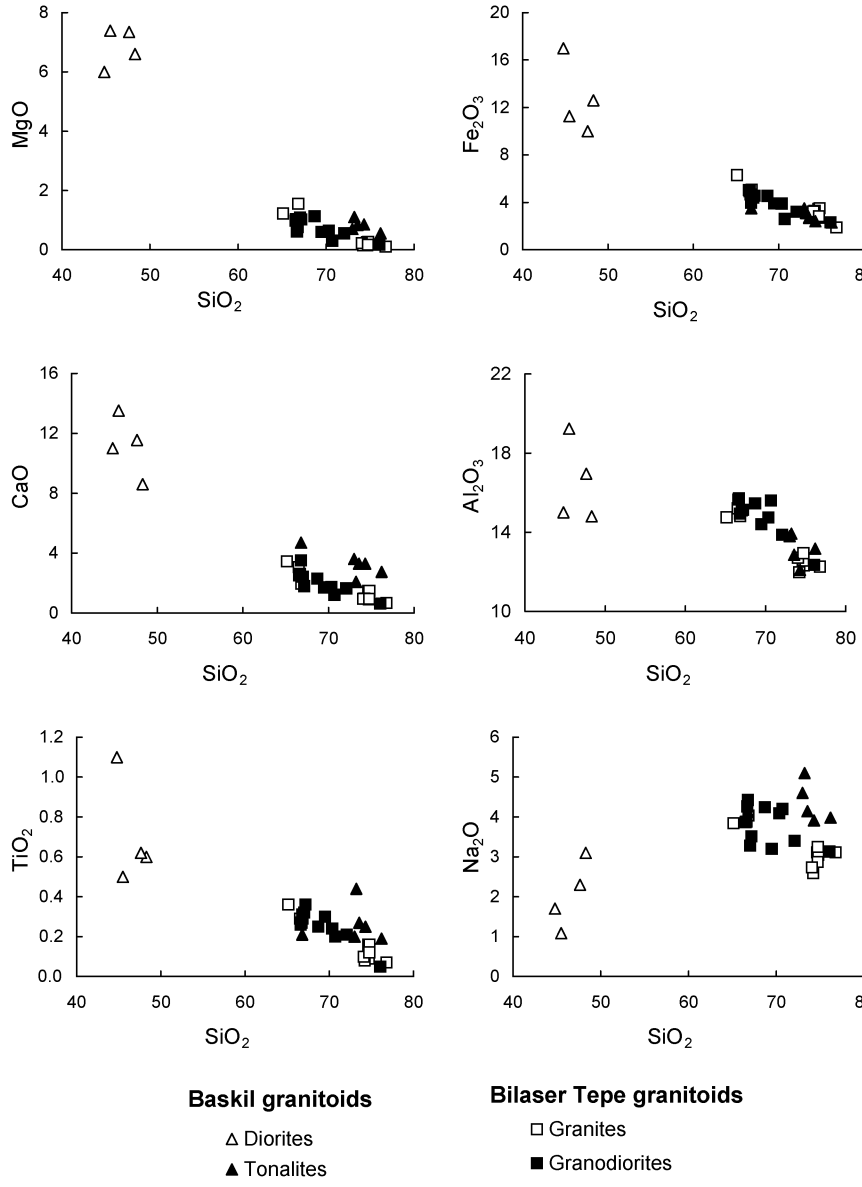

FIG. 8. SiO_2 variation diagrams for the selected major oxides of the Baskil and Bilaser Tepe granitoids.

0.51–2.12; MgO/Fe_2O_{3t} = 0.05–0.31, and MgO/MnO = 3–28. These are characteristics of continental arc-granites (CAG), as described by Maniar and Piccoli (1989).

Trace- and rare-earth element geochemistry

Selected trace-element analyses are given in Table 3 and are plotted against SiO_2 in Figure 10. The Sr, Ba, Zr, and Y concentrations of the Bilaser Tepe granitoids decrease regularly with increasing SiO_2, possibly indicating removal of Ca-plagioclase, biotite, amphibole, and garnet.

Primitive mantle–normalized spidergrams (Sun and McDonough, 1989) of the Baskil and Bilaser Tepe granitoids are given in Figures 11 and 12. The patterns for the Bilaser Tepe granitoids all peak at

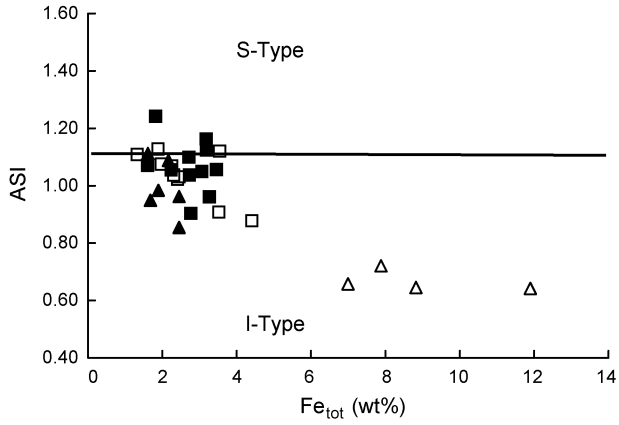

FIG. 9. Relationship between ASI and Fe_{tot} of the Baskil and Bilaser Tepe granitoids (Norman et al., 1992). Symbols are the same as those in Figure 4.

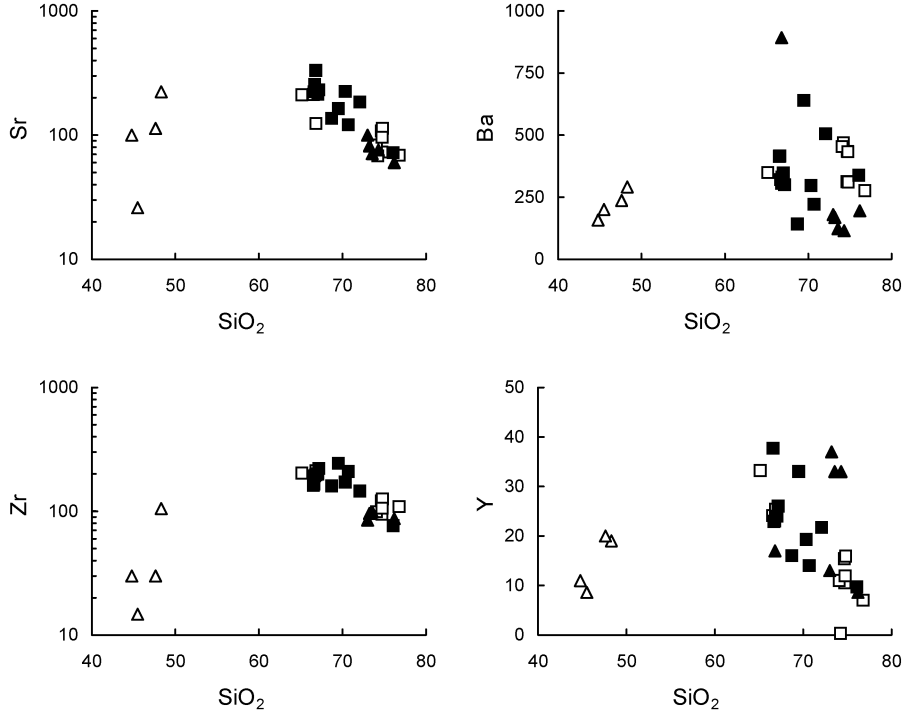

FIG. 10. SiO_2 variation diagrams for selected trace elements of the Baskil and Bilaser Tepe granitoids. Symbols are the same as those in Figure 4.

K, Rb, Th, and U, and all show negative Nb, Ti, and P anomalies (Figs. 11A and 11B). Typical features including enrichment in Ba, Th, Pb and U and depletion in Nb, Ta and Ti, are the characteristic of subduction-related magmas and crustal contamination processes (Gill, 1981; Fitton et al., 1988; Saunders et al., 1988; Thompson et al., 1983; Wilson, 1989), insofar as Nb and Ta are highly sensitive to

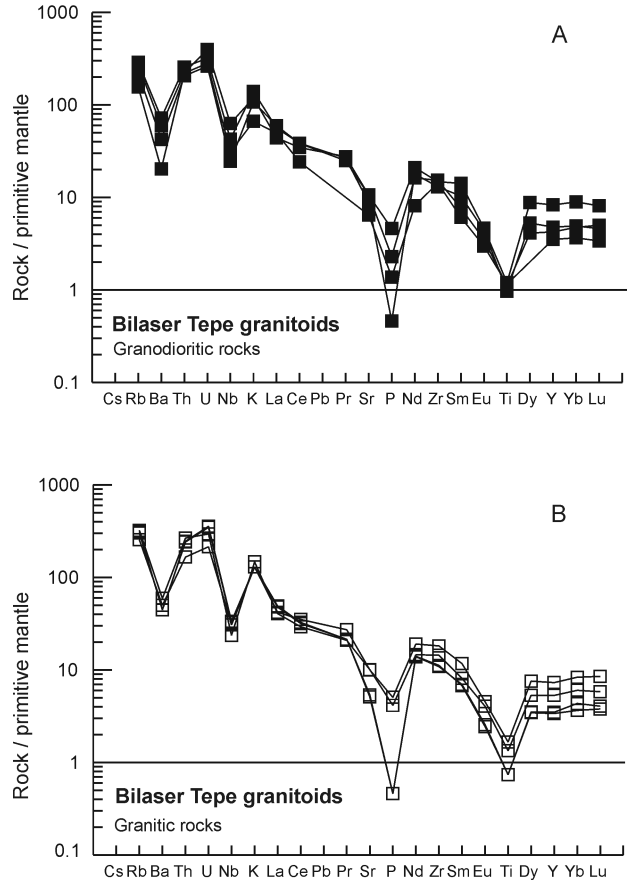

FIG. 11. Primitive mantle–normalized (Thompson, 1982) incompatible trace-element patterns for representative samples from the (A) granodioritic rocks and (B) granitic rocks of the Bilaser Tepe granitoids.

crustal contamination. In addition to these criteria, Ba/Ta and Ba/Nb ratios are used to distinguish the tectonic affinities of magmas. High Ba/Ta (>450) and Ba/Nb (>28) ratios are the most diagnostic geochemical features of island-arc magmas (Gill, 1981; Fitton et al., 1988). Ba/Ta and Ba/Nb ratios of the Bilaser Tepe granitoids range from 173 to 334, and from 6 to 31, respectively. These variations can be attributed to the role of crustal contamination in the evolution of Bilaser Tepe granitoids. On the other hand, a dioritic sample from the Baskil granitoids has very high Ba/Ta (500.5) and Ba/Nb (182) ratios, indicative of a significant subduction component. The abundance patterns (Fig. 12) of representative samples from the Baskil granitoids are characterized by significant Nb negative anomalies relative to the Bilaser Tepe granitoids. This can be interpreted as a mantle source carrying subduction signatures. The Rb/Sr ratios for the Bilaser Tepe and Baskil granitoids are also variable. For instance, Baskil granitoids have lower Rb/Sr ratios (<0.54) than Bilaser Tepe granitoids (Rb/Sr = 0.60–3.04).

Representative REE analyses are listed in Table 3, and chondrite-normalized REE (Nakamura, 1974) patterns for the Bilaser Tepe and Baskil granitoids have been plotted in Figures 13 and 14. Rare-earth element patterns (Figs. 13A and 13B) for selected samples from Bilaser Tepe granitoids exhibit light-REE (LREE) enrichment relative to chondrites (Nakamura, 1974). REEs in the Bilaser Tepe granitoids are fractionated: chondrite-normalized $(La/Yb)_N$ (Thompson, 1982) ratios are between 4.60 and 14.19, whereas Q-diorite and tonalite from Baskil granitoids have restricted and very low $(La/Yb)_N$ ratios (1.15–2.41), suggesting an unfractionated nature. A strong Eu anomaly is present in the

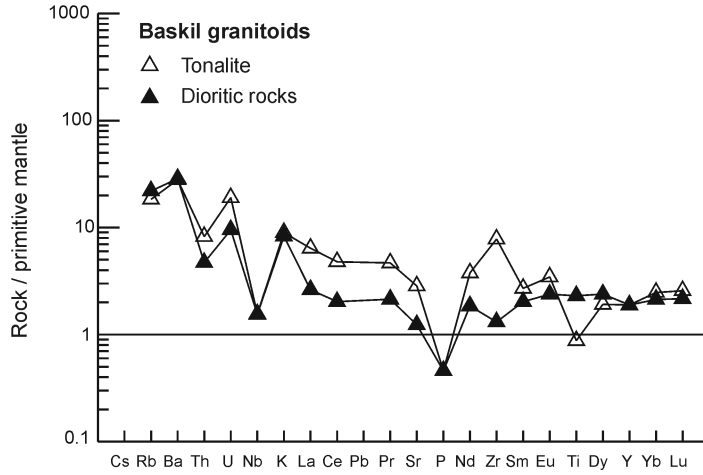

FIG. 12. Primitive mantle–normalized (Thompson, 1982) incompatible trace- element patterns for representative samples from the Baskil granitoids.

Bilaser Tepe granitoids, reflecting the early separation of plagioclase (and alkali feldspar) from the melt, or their accumulation in the restite (Karapetian et al., 2001). The Baskil granitoids differ from others in having smooth profiles for both HREE and LREE, but without Eu anomalies (Fig. 14). As is clear from the spidergrams, enrichment in all incompatible trace elements is considerably higher in the Bilaser Tepe granitoids than those in the Baskil granitoids.

Discussion

As a result of plate convergence and continental collision, extensive magmatism occurred in the Malatya-Elazig area during Late Cretaceous to Pliocene time (Şengör and Yilmaz, 1981). In the study area, oceanic crust formed between the northern margin of the Bitlis-Pütürge massif and the Keban metamorphics during the Early Jurassic to Early Cretaceous (Yazgan, 1984; Asutay, 1985). The extensional regime became a compressional regime beginning in the early Turonian. As a result of compression, the southern branch of the Neo-tethys ocean floor was subducted beneath the Keban microcontinent, leading to the development of arc magmatism (Baskil magmatism) during the Coniacian–Santonian (Yazgan, 1981). Continental collision began immediately after the initiation of arc magmatism. This collision occurred between the Keban microcontinent and the Bitlis-Pütürge massif. Ophiolitic units (Ispendere, Kömürhan, and Guleman ophiolites) were emplaced along the southern margin, which was passive at that time, and collisional granitoids (syn-COLG) developed as a result of crustal thickening (Yazgan et al., 1987; Herece et al., 1992). During the Maastrichtian, post-collisional granitoids (Bilaser Tepe magmatic rocks) developed. The Baskil granitoids probably developed as a result of plate convergence between the Keban microcontinent and the southern branch of the Neo-tethys during Late Cretaceous.

The geochemical data are also consistent with the geodynamic model for the Baskil and Bilaser Tepe magmatism. The Rb vs. Y+Nb and Ta vs Yb discrimination diagrams of Pearce et al. (1984) provide useful constraints concerning the source characteristics for these granitoids (Figs. 15A and 15B). It is apparent that all samples from the Baskil granitoids clearly plot in the volcanic-arc granitoids field (VAG). But most of the samples from the Bilaser Tepe granitoids tend to be shifted from the VAG field to the within-plate granitoid (WPG) and syn-collisional granitoid (syn-COLG) fields (Figs. 15A and 15B). According to Pearce et al. (1984) and Pearce (1996), the petrogenetic discrimination of post-collisional granitoids remains controversial, because it is difficult to distinguish post-collisional granites from volcanic-arc granites on the basis of geochemical data. Thus, this group of granitoids represents a major problem in all tectonic-geochemical classifications of granites. Unlike granites from other settings, the source regions and features of post-collisional granites are controversial and are

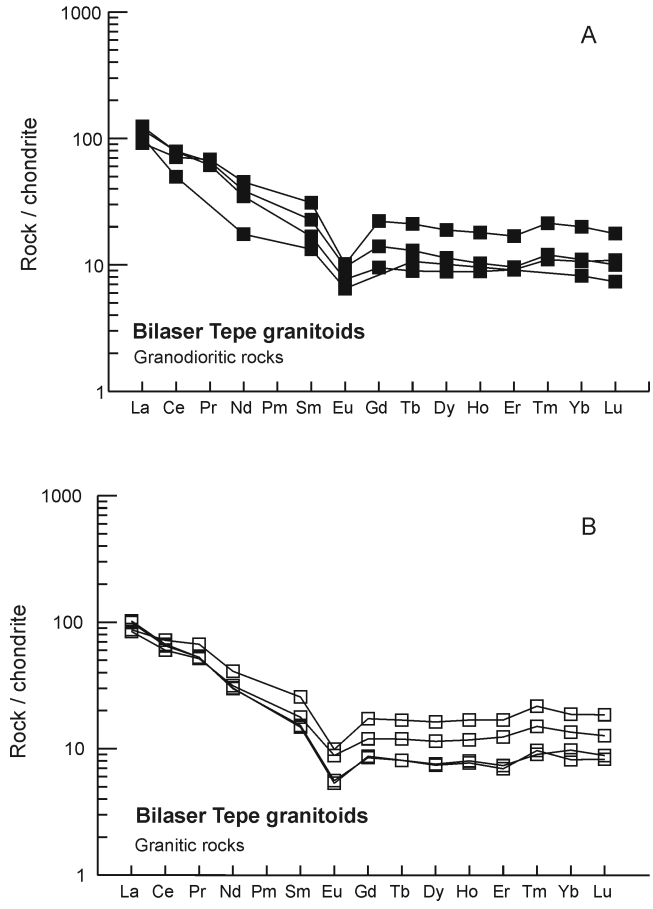

FIG. 13. Chondrite-normalized (Nakamura, 1974) REE patterns for representative samples from the (A) granodioritic rocks and (B) granitic rocks of the Bilaser Tepe granitoids.

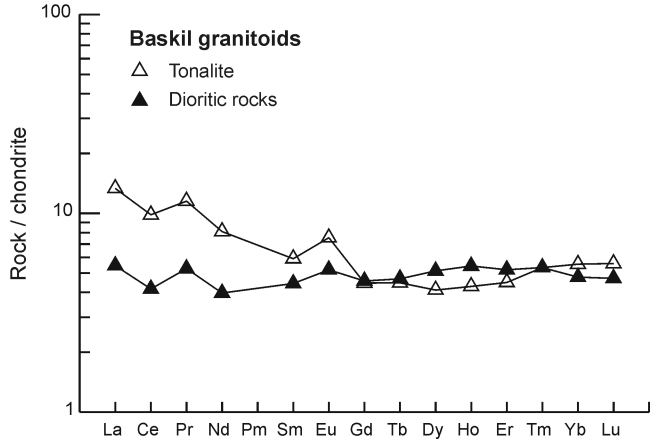

FIG. 14. Chondrite-normalized (Nakamura, 1974) REE patterns for representative samples from the Baskil granitoids.

much more complicated than others. In particular, the source of post-collisional granitoids can be generated by partial melting of lower crust due to thermal relaxation following collision and/or by partial melting of the upper mantle (Pearce et al., 1984). Furthermore, post-collisional magmatism can retain an earlier subduction signature (low Nb, Ta, and Ti; high Th, U, and Pb contents), even though clearly generated in an extensional setting (Alici et al., 1997, 1998, 2004).

The ternary plot for Rb-Ba-Sr (Fig. 16) reflects division of the studied samples into two discrete geochemical types, namely the Rb-rich Bilaser Tepe granitoids relative to the Baskil granitoids. The diagram has also been used to distinguish I-type granites from S-type granites (Tauson, 1974; Karapetian et al., 2001). It is apparent from the figure that most of the samples from the Bilaser Tepe granitoids plot at or near the intersection of the I- and S-type granite fields, whereas the Baskil granitoids clearly plot in the I-type granite field.

According to Taylor and McLennan (1985), Th/U ratios are the most diagnostic features for magmatic melts contaminated by crustal materials. High Th/U ratios in the Bilaser Tepe granitoids thus may indicate the contribution of crustal materials in their evolution (Fig. 17). Conversely, low Th/U ratios (1.75–2.00) in the Baskil granitoids do not support the role of crustal contribution but, as mentioned above, high Ba/Ta (500.5–977) and Ba/Nb (182–176.04) ratios observed in the Baskil granitoids are good indicators of a significant subduction component. Therefore, negative Nb and Ti anomalies in the Baskil and Bilaser Tepe granitoids can be attributed to subduction and crustal contamination, respectively.

Consequently, on the basis of the geochemical features of the Baskil and Bilaser Tepe granitoids, two distinct types of granitoids have been recognized. With regard to trace elements, the Bilaser Tepe granitoids are characterized by high Rb/Sr ratios, fractionated LREE with flat HREE, high LREE/HREE ratios, and significant negative Nb, Ti, Ba, and Eu anomalies. Conversely, the Baskil granitoids are characterized by low Rb/Sr ratios, unfractionated LREE with a roughly positive slope for the HREE, the presence of Nb and Ti anomalies, and a lack of negative Ba and Eu anomalies. Furthermore, the Baskil granitoids clearly demonstrate the characteristic features of I-type arc magmatism on the Rb-Ba-Sr and tectonic discrimination diagrams, suggesting derivation from an island-arc

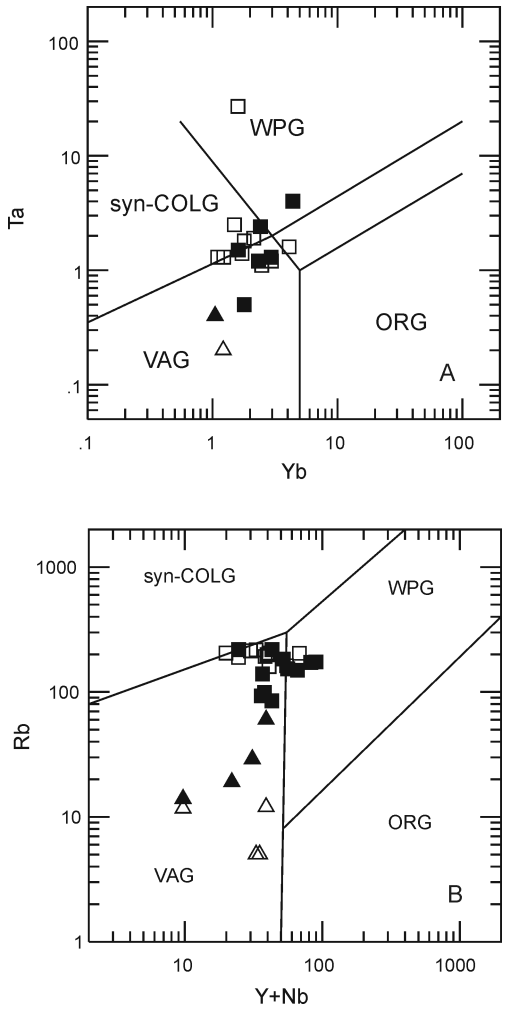

FIG. 15. (A) Ta-Yb and (B) Rb-Y+Nb discrimination diagrams (Pearce et al., 1984) for the Baskil and Bilaser Tepe granitoids. Symbols are the same as those in Figure 4.

setting. The Bilaser Tepe granitoids, on the other hand, have post-collisional geochemical features and show both I- and S-type affinities. These granitoids differ from the Baskil granitoids in their trace-element and REE contents and in their Rb/Sr, Ba/Ta, and Ba/Nb ratios, clearly indicating different source characteristics. Therefore, we suggest that the Bilaser Tepe granitoids were likely produced by melting of a mantle source and underwent crustal contamination during ascent to the surface.

Consequently, the geodynamic evolution of the study area has played an influential role in the

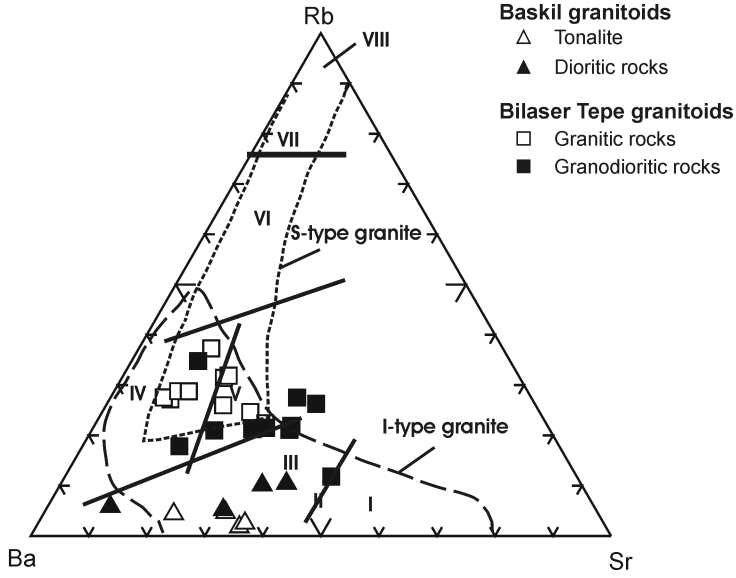

FIG. 16. Rb-Sr-Ba ternary diagram for the Baskil and Bilaser Tepe granitoids (Karapetian et al., 2001). I = plagiogranites of the tholeiitic series; II = granite-granodiorites of the calc-alkaline series; III = subalkaline granites of the latite series; IV = ultrametamorphic granites; V = calc-alkaline granites; VI = plumasitic leucogranites; VII = peralkaline granites; VIII = peralkaline granites-alaskites. S- and I-type granite fields are also shown.

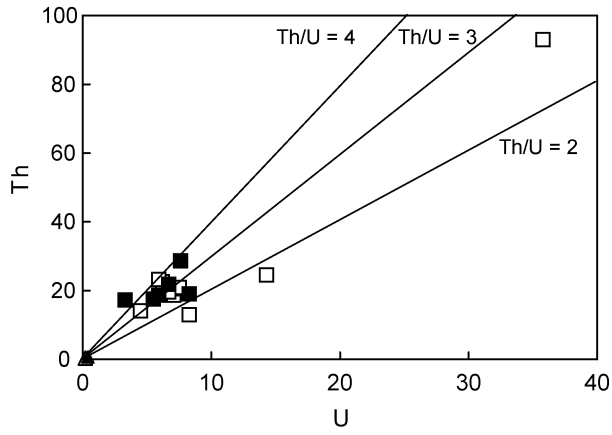

FIG. 17. Th vs. U diagram for the Baskil and Bilaser Tepe granitoids. Symbols are the same as those in Figure 4.

genesis and evolution of the Baskil and Bilaser Tepe magmatic rocks. Based on the geochemical data, together with tectonic discrimination diagrams and the regional geodynamic framework, we conclude that the Baskil and Bilaser Tepe granitoids are consistent with a collision-related magmatic setting.

Conclusions

Based on field, petrologic, and geochemical studies, Late Cretaceous magmatism in the Malatya-Elazig area of the eastern Tauride belt has been differentiated into two distinct groups; namely, the

Bilaser Tepe granitoids with both I- and S-type affinities, and the Baskil granitoids with a significant I-type affinity. The Bilaser Tepe granitoids are peraluminous to metaluminous (A/CNK = 0.88–1.24), are characterized by high K_2O/Na_2O (generally greater than 1) and Th/U, and low Ba/Ta and Ba/Nb ratios, and plot as syn-COLG (S-type) and VAG (I-type) on tectonic discrimination diagrams. The Baskil granitoids are generally metaluminous (A/CNK = 0.64–0.98) to slightly peraluminous (A/CNK = 1.09–1.11), are characterized by low K_2O/Na_2O (<0.65) and Th/U, and high Ba/Ta and Ba/Nb ratios, and plot as VAG (I-type) on tectonic discrimination diagrams.

Acknowledgements

This study was supported by the General Directorate of MTA in the framework of the "GAP Mineral Exploration Project" during 1992–1996. We are extremely grateful to the late Şahin Tüfekçi, who was the project manager, especially for his help during a field excursion. We extend our special appreciation to Dr. Tandogan Engin, Selahattin Yildirim, Prof. Dr. Taner Ünlü, and Dr. Evren Yazgan for their valuable and constructive comments. Dr. Steve Mittwede and Bülent Bayburtoglu are thanked for improving the English exposition. We would also like to thank Sabriye Metin for her assistance with computer analysis.

REFERENCES

Akgül, M., 1991, Petrographical and petrological features of Baskil (Elazig) granitoids: Yerbilimleri Geosound, v. 18, p. 67–78.

Akgül, B., and Bingöl, F. A., 1997, Petrographical and petrological features of magmatic rocks in the the vicinity of Piran village (Keban), *in* Yearbook of the Geological Engineering Department of the University of Selçuk, p. 13–24 (in Turkish).

Alici, P., Temel, A., Gourgaud, A., Kieffer, G., and Gündogdu, M. N., 1997, Petrology and geochemistry of Lower Pliocene alkaline volcanism in the Gölcük area (Isparta, SW Turkey) [abs]: EUG 10, Terra Abstracts, abstracts supplement, No. 1, Terra Nova, Vol. 9.

Alici, P., Temel, A., Gourgaud, A., Kieffer, G. and Gündogdu, M. N., 1998, Petrology and geochemistry of potassic rocks in the Gölcük area (Isparta, SW Turkey): Genesis of enriched alkaline magmas: Journal of Volcanology and Geothermal Research, v. 85, nos. 1–4, p. 423–446.

Alici Şen, P., Temel, A., and Gourgaud, A., 2004, Petrogenetic modelling of Quaternary post-collisional volcanism: A case study of central and eastern Anatolia: Geological Magazine, v. 141, no. 1, p. 1–18.

Asutay, H. J., 1985, Geological and petrological investigation of around Baskil (Elazig): Unpubl. Ph.D. thesis, Ankara University, Graduate School of Natural and Applied Sciences, Ankara, Turkey, 156 p.

Asutay, H. J., 1988, Geology of the Baskil (Elazig) area and petrology of Baskil magmatics: Bulletin of the Directorate of Mineral Research and Exploration, v. 107, p. 49–72.

Asutay, H. J., and Turan, M., 1986, Geology of the Keban-Baskil (Eastern Taurus): Ankara, Turkey, Directorate of Mineral Research and Exploration, Unpubl. report no: 8008 (in Turkish).

Beyarslan, M., 1991, Petrographical features of Ispendere Ophiolite (Malatya-Turkey): Unpubl. M.S. thesis, Firat University, Graduate School of Science and Technology, Elazig, Turkey, 57 p.

Bingöl, A. F., 1984, Geology of the Elazig area in the Eastern Taurus region, *in* Tekeli, O., and Göncüoglu, M. C., eds., Geology of the Taurus Belt: Ankara, Turkey, Directorate of Mineral Research and Exploration, p. 209–216.

Bingöl, A.F., 1988, Petrographical and petrological featural setting on the intrusive rocks of Yüksekova Complex in the Elazig region (Eastern Taurus-Turkey): Journal of Firat Univ., v. 3, no. 2, p. 1–17.

Debon, F., and Le Fort, P., 1988, A cationic classification of common plutonic rocks and their magmatic associations: Principles, methods, applications: Bulletin of Mineralogy, v. 111, p. 493–510.

Dumanlilar, H., 1998, Investigation of mineralization around Ispendere (Malatya): Unpubl. M.Sc. thesis, Ankara University, Graduate School of Natural and Applied Sciences, Ankara, 132 p.

Dumanlilar, H., Aydal, D., and Dumanlilar, Ö., 1999, Geology, mineralogy and geochemistry of sulphide mineralization of the Ispendere region (Malatya): Bulletin of the Directorate of Mineral Research and Exploration, v. 121, p. 225–250.

Dumanlilar, Ö., 1993, Geology and petrography of the magmatic rocks around Ispendere (Malatya): Unpubl. M.S. thesis, Ankara University, Graduate School of Natural and Applied Sciences, Ankara, Turkey, 62 p.

Dumanlilar, Ö., 2002, Investigation of the mineralization related to the granitic rocks in Baskil (Elazig): Unpubl. Ph.D. thesis, Ankara University, Graduate School of Natural and Applied Sciences, Ankara, Turkey, 196 p.

Fitton, J. G., James, D., Kempton, P. D., Ormerod, D. S., and Leeman, W. P., 1988, The role of lithospheric mantle in the generation of late Cenozoic basic magmas in the Western United States: Journal of Petrology, Special Lithosphere Issue, p. 331–349.

Fytikas, M., Innocenti, F., Manetti, P., Peccerillo, A., and Villari, L. 1984, Tertiary to Quaternary evolution of volcanism in the Aegean region, *in* Dixon, J. E., and Robertson, A. H. F., eds., The geological evolution of the Eastern Mediterranean: Geological Society of London, Special Publication, v. 17, p. 687–699.

Gill, J. B., 1981, Orogenic andesites and plate tectonics: New York, NY, Springer-Verlag.

Herece, E., Akay, E., Küçümen, E., and Sariaslan, M., 1992, Geology of Elazig-Sivrice-Palu region: Ankara, Turkey: Directorate of Mineral Research and Exploration, unpubl. report no: 9634 (in Turkish).

Irvine, T. N., and Baragar, W. R. A., 1971, A guide to the chemical classification of the common volcanic rocks: Canadian Journal of Earth Science, v. 8, p. 523–548.

Karapetian, S. G., Jrbashian, R. T., and Mnatsakanian, A. Kh., 2001, Late collision rhyolitic volcanism in the north-eastern part of Armenian Highland: Journal of Volcanology and Geothermal Research, v. 112, p. 189–220.

Maniar, P. D., and Piccoli, P. M., 1989, Tectonic discrimination of granitoids: Geological Society of America Bulletin, v. 101, p. 635–643.

MTA (Directorate of Mineral Research and Exploration), 2002, 1:500,000 scale geological maps of Turkey, Sivas sheets.

Nakamura, N., 1974, Determination of REE, Ba, Fe, Mg, Na and K in carbonaceous and ordinary chondrites: Geochimica et Cosmochimica. Acta, v. 38, p. 757–775.

Norman, M. D., Leeman, W. P., and Mertzman, S. A., 1992, Granites and rhyolites from the northwestern USA: Temporal variation in magmatic processes and relations to tectonic setting: Transactions of the Royal Society of Edinburgh, Earth Science, v. 83, p. 71–81.

Özgül, N., 1981, Geology of Munzur Mountain: Ankara, Turkey, Directorate of Mineral Research and Exploration, unpubl. report no. 6995 (in Turkish).

Pearce, J. A., 1996, Sources and settings of granitic rocks: Episodes, v. 19, p. 4.

Pearce, J. A., Harris, N. B. W., and Tindle, A. G., 1984, Trace element discrimination diagrams for the tectonic interpretation of granitic rocks: Journal of Petrology, v. 25, p. 956–983.

Perinçek, D., 1979, The geology of Hazro-Korudag-Çüngüş-Maden-Ergani-Hazar-Elazig-Malatya area: Guide Book, Türkiye Jeoloji Kurumu Yayini, 33 p.

Saunders, A. D., Norry, M. J. and Tarney, J., 1988, Origin of MORB and chemically-depleted mantle reservoirs: Trace element constraints: Journal of Petrology, Special Lithosphere Issue, p. 415–445.

Sun, S. S., and McDonough, W. F., 1989, Chemical and isotopic systematics of oceanic basalts: Implications for mantle composition and processes, *in* Saunders, A. D., and Norry, M. J., eds., Magmatism in ocean basins: Geological Society of London, Special Publication, v. 42, p. 313–345.

Streckeisen, A., 1976, To each plutonic rock, its proper name: Earth Science Review, v. 12, p. 1–13.

Şengör, A. M. C., 1980, Türkiye'nin neotektoniginin esaslari (Fundamentals of the neotectonics of Turkey): Türkiye Jeoloji Kurumu Konferans serisi, v. 2, p. 40.

Şengör, A. M. C., and Yilmaz, Y., 1981, Tethyan evolution of Turkey: A plate tectonic approach: Tectonophysics, v. 75, p. 181–241.

Tauson, L. V., 1974, Geochemical types and potential ore-bearing granitoids: Moscow, USSR, Nauka, 279 p. (in Russian).

Taylor, S. R., and McLennan, S. M., 1985, The continental crust: Its composition and evolution: An examination of the geochemical record preserved in sedimentary rocks. Oxford, UK, Blackwell Scientific Publications, 46 p.

Thompson, R. N., 1982, British Tertiary volcanic province: Scottish Journal of Geology, v. 18, p. 49–107.

Thompson R. N., Morrison M. A., Dickin A. P., and Hendry, G. L., 1983, Continental flood basalts … Arachnids rule OK?, *in* Hawkesworth, C. J., and Norry, M. J., eds., Continental basalts and mantle xenoliths: Nantwich, UK, Shiva, p. 158–185.

Turan, M., 1984, The stratigraphy and tectonic of the Baskil-Aydinlar (Elazig): Unpubl. Ph.D. thesis, Firat University, Graduate School of Science and Technology, Elazig, Turkey, 180 p.

Turan, M., Aksoy, E. and Bingöl, F. A., 1995, The features of geodinamic evolution of the Eastern Taurides in Elazig region: Firat University, Fen ve Mühendislik Bilimleri Dergisi, v. 7, no. 2, p. 177–199 (in Turkish).

Yazgan, E., 1972, Etude geologique et petrographique du complexe ophiolitique de la region situee au Sud-Est de Malatya et de sa couverture volkano sedimentaire: Unpubl. Ph.D. thesis, Faculte des Sciences de L'universite de Geneve, Department de Mineralogie et Geophysique, these no. 1575-1, 236 p.

Yazgan, E., 1981, Study of active paleo-continent margin in Eastern Taurides (Upper Cretaceous–Middle Eocene): Hacettepe University, Yerbilimleri, v. 7, p. 83–104.

Yazgan, E., 1984, Geodynamic evolution of the Eastern Taurus region, *in* Tekeli, O., and Göncüoglu, M. C., eds., Geology of the Taurus belt: Conference proceedings: Ankara, Turkey: Directorate of Mineral Research and Exploration.

Yazgan, E., Asutay, H. J., Gültekin, M. C., Poyraz, N., Sirel, E., and Yildirim, H., 1987, Geology of southeastern Malatya and geodynamic evaluation of the Eastern Taurides: Ankara, Turkey, Directorate of Mineral Research and Exploration, unpubl. report no. 2268 (in Turkish).

Yazgan, E., and Chessex, R., 1991, Geology and tectonic evolution of the Southeastern Taurides in the region of Malatya: Türkiye Petrol Jeologlari Dernegi Bülteni, v. 3, p. 11–42 (in Turkish).

Yilmaz, Y., Güner, Y., and Şaroglu, F., 1998, Geology of the Quaternary volcanic centres of the east Anatolia: Journal of Volcanology and Geothermal Research, v. 85, nos. 1-4, p. 173–211.

Wilson, M., 1989, Igneous petrogenesis: London, UK, Unwin Hyman Ltd., 465 p.